Correlated electronic structure and chemical bonding of Ce pnictides and γ-Ce

Mikhail S. Litsarev,[1] Igor Di Marco,[1] Patrik Thunström,[1] and Olle Eriksson[1]

[1] *Department of Physics and Astronomy, Uppsala University, Box 516, SE-75120, Uppsala, Sweden*

(Dated: September 4, 2012)

We present calculated spectral properties and lattice parameters for cerium pnictides (CeN, CeP, CeAs, CeSb, CeBi) and γ-Ce, within the LDA/GGA+DMFT (local density approximation/generalized gradient approximation + dynamical mean field theory) approach. The effective impurity model arising in the DMFT is solved by using the spin-polarized T-matrix fluctuation-exchange (SPTF) solver for CeN compound, and the Hubbard I (HI) solver for CeP, CeAs, CeSb, and CeBi. For all the addressed compounds the calculated spectral properties are in reasonable agreement with measured photoelectron spectra at high binding energies. At low binding energies the HI approximation does not manage to capture the Kondo-like peak observed for several of the Ce-pnictides. Nevertheless, the calculated lattice constants are in a good agreement with available experimental data, showing that the such a peak does not play a major role on the bonding properties. Furthermore, the HI calculations are compared to a simpler treatment of the Ce $4f$ electron as core-like in LDA/GGA for CeP, CeAs, CeSb, and CeBi, and the two approaches are found to give similar results.

PACS numbers: 71.20.Eh, 71.15.Nc, 71.28.+d, 71.15.Mb

I. INTRODUCTION

Cerium monopnictides, CeX, where X = (N, P, As, Sb, Bi) form in a rock-salt type crystal structure. In this structure the Ce atom is located on an fcc Bravais lattice, with the pnictogen atoms entering octahedral voids of this lattice. Hence, the position of the Ce atoms in the Ce pnictides is the same as for the α and γ phase of elemental cerium, which has attracted so much attention due to its isostructural volume collapse[1–3]. The possibility of tuning the $4f$ wave function overlap between the cerium atoms is an opportunity in the Ce pnictides, since the pnictogen atoms all have different size, and hence they expand the fcc lattice to different degrees. This offers a possibility to in a more detailed way investigate localization – delocalization transitions in Ce based materials.

The Ce pnictides have indeed been studied intensively in the past, due to that they display several unique and interesting properties, which will shortly be reviewed below. The lattice constants have been determined, and they suggest that the electronic structure and chemical bonding of CeN stand out as being different from the rest of the series[4,5]. This has previously been suggested to be caused by itinerant $4f$ states for CeN[6,7], and the theoretical interpretation[8] of the measured optical properties are in line with this reasoning[9]. The heavier Ce pnictides have lattice constants, and other physical properties, which suggest a localized and non-bonding $4f$ shell. The observed properties of the heavier Ce pnictides are in many ways unique, for instance, the magnetism and the crystal field splitting of the $4f$ shell exhibit puzzling behaviour, as analyzed in detail in Refs. 10–14.

Another unique feature of the Ce pnictides is found in the excited state properties, as revealed by the x-ray photoelectron spectroscopy (XPS). Several investigations have been reported[15–21], and they reveal an XPS spectrum which is rather complex as concerns the $4f$ signal. A feature between 2.9 - 3.2 eV binding energy is observed together with a feature closer to the Fermi level, at around 0.6 eV binding energy. The exact positions of these two distinct features vary from pnictide to pnictide, see e.g. Ref. 16 and 17. The presence of these two peaks is at first glance surprising, having in mind that a localized f^1 configuration of the heavier Ce pnictides, is expected to result in one spectral feature corresponding to a $f^1 \rightarrow f^0$ transition. However, it has been pointed out[17,22] that two screening channels of the final state core hole are possible for this excitation, a well screened and a poor screened channel, which results in two distinct spectral features. The presence of two peaks in the $4f$ spectrum is a property not only of Ce pnictides, but also other Ce compounds (see, for example, Refs. 23–27).

On the theoretical side, electronic structure calculations have been published for CeN, analyzing the energy band structure and the optical properties[8]. Results of this work are based on the LDA/GGA and, essentially, correlation effects are taken into account only weakly. A recent calculation[28] for CeN focused on the electronic structure and the lattice dynamics. In this work the $4f$ states were considered as delocalized, and the calculations used both the LDA/GGA level of approximation as well as the so called GW[29] approximation. For the heavier Ce pnictides a theory of the crystal field splitting was proposed[30], which successfully reproduced the observations of Ref. 10. The work of Ref. 30 was a combination of model considerations and first principles theory, in which the localization of the $4f$ wave function was enforced in the calculation, and then the hybridization to other valence states was estimated from this electronic configuration.

Previous DMFT investigations of Ce pnictides are presented in Refs. 31–33, wherein the Anderson impurity problem was solved in a finite-U extension of the non-

TABLE I. Muffin-Tin radii (in atomic units) of the cerium and pnictogen atoms used in the present calculations.

	CeN	CeP	CeAs	CeSb	CeBi
R_{MT}(Ce)	2.45	2.75	2.83	2.90	2.89
R_{MT}(X)	2.10	2.40	2.50	2.90	2.91

TABLE II. Experimental binding energies (ΔE) and DC terms for the $4f$ states of cerium in the Hubbard I approximation.

	CeP	CeAs	CeSb	CeBi
ΔE (eV)	2.95	3.05	3.0	3.2
PW91, DC (Ry)	0.335	0.308	0.262	0.247
PBE96, DC (Ry)	0.344	0.316	0.270	0.255
AM05, DC (Ry)	0.356	0.328	0.283	0.269

crossing approximation (NCA), including some lowest-order crossing diagrams.

In the present paper we revisit the problem of the electronic structure of the Ce pnictides, and the localization-delocalization phenomena of the $4f$ shell, in light of recent developments of treating electron correlations directly in electronic structure calculations. In particular, we investigate how well dynamical mean field theory reproduces the lattice parameters and spectral properties of these materials, and we have used the implementation reported in Refs. 34–37 for these purposes, with the HI and SPTF solvers.

II. COMPUTATIONAL DETAILS

The calculations presented in this work are based on the density functional theory (DFT)[38,39] combined with the dynamical mean-field theory[40–44] method. The DFT calculations were done in the local-density approximation with exchange-correlation functional PW91[45], and in the generalized gradient approximation using the PBE96[46] parametrization, as well as with the AM05 functional[47], within the full-potential linearised muffin-tin orbitals (FP-LMTO) approach[30,48,49]. The LDA/GGA+DMFT calculations were done by means of the implementation presented in Refs. 34–37, with the total energies evaluated following Ref. 35. To solve the Anderson impurity model arising in the DMFT part, the SPTF solver[34,50,51] was used for CeN, whereas the Hubbard I solver[36,40,52] was used for CeP, CeAs, CeSb, and CeBi.

TABLE III. Calculated and experimental lattice parameters of cerium pnictides in atomic units.

	CeN	CeP	CeAs	CeSb	CeBi
PW91, $4f$-itinerant	9.38	10.73	11.01	11.72	11.96
PBE96, $4f$-itinerant	9.55	10.94	11.26	12.00	12.27
AM05, $4f$-itinerant	9.42	10.78	11.09	11.81	12.07
PW91, $4f$-core	9.79	11.08	11.31	11.92	12.10
PBE96, $4f$-core	9.98	11.32	11.59	12.24	12.57
AM05, $4f$-core	9.86	11.17	11.41	12.03	12.20
PW91+DMFT	9.38	11.09	11.32	11.95	12.13
PBE96+DMFT	9.56	11.30	11.55	12.22	12.44
AM05+DMFT	9.43	11.19	11.43	12.06	12.25
Experiment	9.49	11.20	11.49	12.13	12.26

The LDA/GGA+DMFT scheme was applied to the $4f$ state of cerium using two types of the correlated orbitals[34]: orthogonalized LMTO subspace (ORT) and muffin-tin only correlated subspace (MT). All these ORT and MT orbitals are localized, and form orthonormal sets. The ORT set consists of functions obtained from the FP-LMTO method with the LDA/GGA Hamiltonian for the correlated states. The MT correlated subspace is defined only into the muffin-tin region, and outside of the muffin-tin spheres the MT orbitals are taken equal to zero by definition. Properties of these subspaces are analyzed in the works published in Refs. 34 and 53. In the present calculations the MT set was used for CeN, and the ORT set for all other Ce pnictides.

The LDA/GGA calculations included spin-orbit coupling in the scalar-relativistic approximation, and only within the muffin-tin spheres. The radii of the muffin-tin spheres for the different compounds were kept constant while changing the lattice parameters, and their values are reported in Table I. For the Brillouin zone integration the tetrahedron method was used with a $16\times16\times16$ **k**-mesh. It corresponds to 85 **k**-points in the irreducible wedge of the Brillouin zone with the total number of **k**-points in the Brillouin zone equal to 2048. For the charge density and potential angular decomposition inside the muffin-tin spheres the value of maximum angular momentum was taken equal to $l_{\max} = 8$. Three kinetic energy tails were used, corresponding to $\{-0.3, -2.3, -1.6\}$ Ry. Finally all calculations were non-spin polarized, except CeN which was converged to a ferromagnetic solution. Magnetic properties were in fact considered at the DMFT level, and the SPTF solver works better when starting from a magnetic solution[54].

Calculations without DMFT in the pure PW91/PBE96/AM05 approximations were done in two ways: the cerium $4f$ electrons were treated either as core or as itinerant states. In the latter case two kinetic energy tails were considered for the basis.

For the LDA/GGA+DMFT calculations it is necessary to choose an adequate value for the Hubbard and (Hund) exchange parameters U and J. For all Ce pnictides except CeN we have used U=7 eV and J=0.95 eV, which is compatible with previous calculations[31] considering that our method is also based on a fully rotationally invariant U-matrix[34]. Conversely the $4f$ states in CeN have basically an itinerant character, as discussed more in detail in the results section. This implies that the

screening of the Coulomb interaction is much more effective and the value of U reduced in comparison to the other Ce pnictides. Following these guidelines and having in mind that the SPTF solver tends to overestimate correlation effects[35,55] we have used U=2 eV, which is consistent with its applicability range. Higher values of U have also been studied but these results have not been reported here as they gave the same physical picture as U=2 eV. The value of the Hund's exchange is less dependent on the nature of the screening in a material, and therefore we have used J=0.95 eV for CeN as well.

To calculate the energy versus volume curves in the Hubbard I approximation, it is important to correctly treat the double counting term H_{DC} included in the local problem[35]. The H_{DC} term is used to remove the wrong contributions of local Coulomb interaction already contained in the DFT Hamiltonian projected on the correlated orbitals ($4f$ states) and used in the DMFT part. The double counting term was first calculated from the HI solver at experimental lattice constants, and then kept fixed for all the other values. In order to fix the main occupied peak at the correct position the photoemission data available from experiments[16,18,19,56] were used. The experimental binding energies and double counting term values are presented in Table II for the PW91/PBE96/AM05 + HI approximations.

CeN did not present these problems since in the SPTF solver the double counting correction can be directly related to a fully hybridizing self-energy by simply removing the orbitally averaged $\Sigma(0)$, separately for each spin channel. When evaluating the local interacting Green's function with the SPTF solver was important to consider a fully renormalized propagator to obtain a conserving approximation in Baym-Kadanoff sense[57–59].

III. RESULTS

The calculated lattice parameters are presented in Table III, where we also show available experimental data[5,61–67]. A selection of these results are plotted in Fig. 1. In this figure we show experimental values of lattice constants and values obtained with AM05 DFT functional combined with the SPTF solver for CeN and with the Hubbard I solver for all other pnictides. An overall good agreement between experimental data and calculations is observed, both concerning the trend as well as the absolute values.

In Fig. 2 we present the calculated lattice constants from different approximations. Results are given for CeN using the SPTF solver with AM05 and PW91 DFT functionals as well as for pure AM05 DFT calculations with the $4f$ electron of Ce atom considered as itinerant. For all other pnictides, results are given for the Hubbard I solver with AM05 and PW91 DFT functionals. The choice of showing in Fig. 2 parametrizations from the AM05 and PW91 functional was made since these two approximations give the best and, respectively, the worst agreement

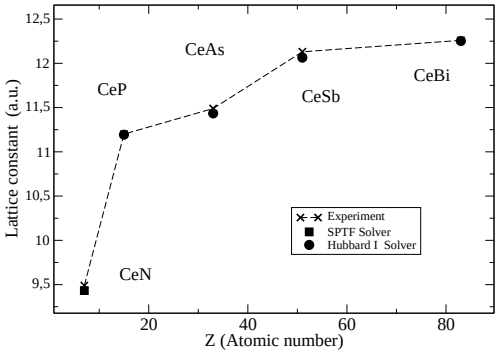

FIG. 1. Experimental and calculated lattice constants of Ce pnictides. The theoretical values for CeN are obtained with the SPTF solver and the AM05 DFT functional. The Hubbard I solver together with the AM05 DFT functional was used for all other pnictides.

with observed lattice parameters. As Fig. 2 shows, the difference between the two functionals, when combined with DMFT, is very small and both parametrizations reproduce observations with good accuracy. In Fig. 2 we also show results from more time efficient calculations, treating the $4f$ states as localized core states and using the AM05 DFT functional. Moreover for CeN a calculation with the same functional and $4f$ states treated as itinerant is showed.

The DFT calculations with $4f$ electrons treated as core states for CeP, CeAs, CeSb and CeBi, give a good agreement with the experimental data. On this level of approximation the $4f$ states do not contribute to the chemical bonding. The Hubbard I calculations also treat the $4f$ states as essentially non-bonding and atomic like, al-

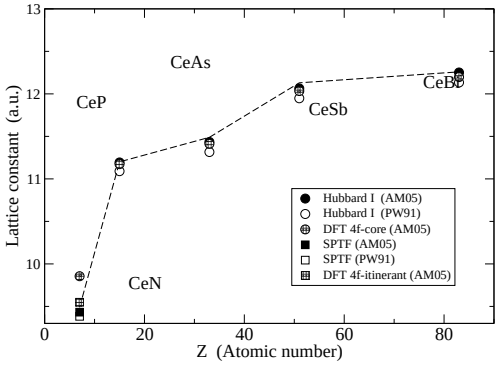

FIG. 2. Calculated lattice constants of Ce pnictides. The theoretical values for CeN are obtained with the SPTF solver and two DFT parametrizations, AM05 and PW91. The Hubbard I solver with both the AM05 and PW91 DFT functionals was used for all other pnictides. These data are compared to calculations using localized $4f$ (core) states with the AM05 and PW91 functional. For CeN the plain AM05 DFT results with $4f$ valence electrons are also reported, emphasizing how such a description is much better than the assumption of localized core states for this material.

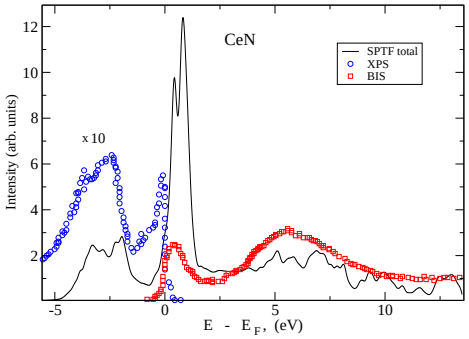

FIG. 3. (Color online) Experimental and calculated spectrum of CeN. The blue points label the XPS data and the red points mark the BIS spectrum from Ref. 68, where the relative intensities of the XPS and BIS spectra have been tentatively adjusted. The factor ($\times 10$) comes directly from Ref. 68, and we have kept it to make a better comparison between the experimental XPS data and the theoretical curve. The solid line denotes the total spectral function using the SPTF solver for the Ce $4f$ states.

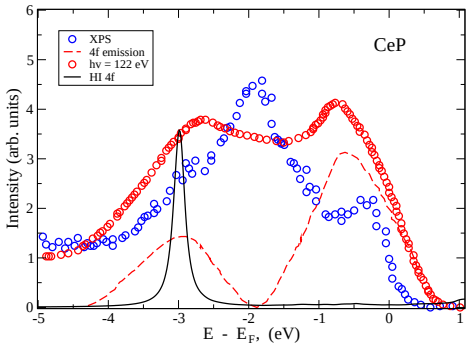

FIG. 4. (Color online) Experimental and calculated spectral properties of the $4f$ states for CeP. The XPS data from Ref. 16 are marked as blue circles. The red circles label the resonant spectrum of CeP, while the red dashed line labels the extracted photoemission spectrum of $4f$ states from Ref. 17. The black solid line is the calculated spectral function of the Ce $4f$ states with the Hubbard I solver.

beit a small degree of hybridization is present in such kind of calculations. All data in Fig. 1 and Fig. 2 point to that the $4f$ states do not contribute to the chemical bonding in the heavier Ce pnictides.

In contrast, the CeN compound is a system which seems best described having delocalized $4f$ states as it follows from the comparison of our calculated values and the experimental data. The DMFT calculation with the SPTF solver and the pure AM05 DFT calculation with itinerant $4f$ states reproduce the observed lattice constant with good accuracy. Conversely if one tries to assume a localized $4f$ electron in the form of a core state the results become more in line with the other Ce pnictides, but the agreement with experiments worsen. These facts point to that the $4f$ states have an important role in the chemical bonding, which results in a significantly smaller lattice constant of CeN in comparison to the heavier Ce pnictides (Fig.1). The delocalized nature of the $4f$ electron makes it not suitable for the Hubbard I approximation or any other approach in the strong coupling limit, unless one wants to apply semi-empirical workarounds. For example, in a previous LDA+DMFT study[31] based on the NCA solver, the $4f$ hybridization function in CeN had to be rescaled of a factor 2 to avoid an unphysical occupation number of the $4f$ shell.

To give further evidence to this fact we observe that the calculated spectral properties of CeN are in rather good agreement with experimental data, when considering the $4f$ states as essentially itinerant with some degree of correlation resulting from the SPTF solver. This comparison is presented in Fig. 3, where both occupied and unoccupied states from the calculations are compared to experimental XPS and BIS data. Note that the calculation of the occupied states reproduce the spectral feature between 3 and 5 eV binding energy, stemming mostly from N p-states, whereas the feature at the Fermi level is dominated by the Ce $4f$ states, which form a band-like feature pinned at the Fermi level. This results in that the unoccupied states have a $4f$ feature at the Fermi level, which is different from the situation for the heavier Ce pnictides, as discussed below. The unoccupied states of CeN also have a broader feature at 5 - 6 eV energy, which is dominated by Ce $5d$ states which hybridize with ligand p states.

In Fig. 4 we present the CeP $4f$ spectral function, which sometimes is loosely referred to as the correlated density of states (DOS) to relate it to the band-structure theory. In this figure we make a comparison to the experimental data from Refs. 16 and 17. As one can see, the Hubbard I approximation describes the deeply localized $4f$ feature in a proper way, although due to life time broadening and finite spectrometer resolution the experimental feature is much wider compared to theory. Note

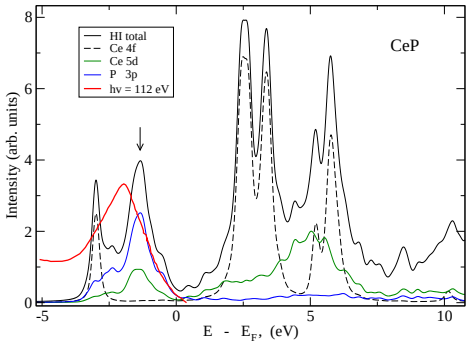

FIG. 5. (Color online) Total spectral function calculated with the Hubbard I solver (black solid line), compared with experimental data from Ref. 17. We also present the projections for the Ce $5d$ and $4f$ states, and the P $3p$ states (dashed lines). The vertical arrow labels the pd peak which is close to the experimental non resonant photoemission data taken at $h\nu = 112$ eV (red solid line).

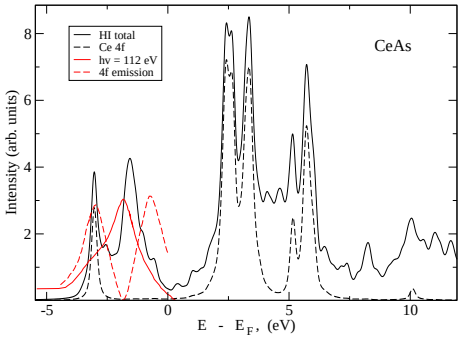

FIG. 6. (Color online) Experimental and calculated spectral properties using Hubbard I approximation of CeAs. The total spectral function is labelled by the black solid line, the Ce $4f$ projection is marked by the black dashed line, while the red dashed line marks the experimental resonant $4f$ emission from Ref. 17. The red solid line represents the experimental data from nonresonant emission (formed by As $4p$ and Ce $5d$ states).

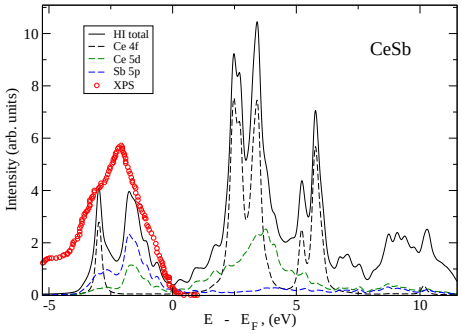

FIG. 7. (Color online) Total spectral function of CeSb calculated with the Hubbard I solver (black solid line), compared with the experimental data from Ref. 16. We also present projections for the Ce $4f$ and $5d$ states, and the Sb $5p$ states (dashed lines). The pd-peak is close to the experimental data from nonresonant photoemission (red circles).

that the Hubbard I approximation is not able to capture the well screened feature at the Fermi level, and indeed the experimental feature can not be reproduced with the present calculations.

The experimental results for the non resonant frequency of $4f$ Ce states are compared with the total and partial theoretical spectral functions in Fig. 5. For this photon energy the main contribution to the observed peak is from cerium $5d$ states and phosphorus $3p$ states[17]. The experimental peak-width and position are reproduced by the Ce $5d$ and P $3p$ partial spectral functions, as Fig. 5 shows.

A similar picture occurs for the other heavy pnictides, for which we in Figs. 6, 7, 8 compare calculated spectral features with experimental data taken on and off resonance. As discussed, the $4f$ feature close to the Fermi energy (the well screened peak) is not reproduced in our Hubbard I calculation. However, going from CeP to CeBi the experimental $4f$ peak at the Fermi level decreases in intensity and becomes almost negligible in the CeBi case. For this pnictide the Hubbard I approximation hence gives the best description of the spectral features.

In Figs. 5, 6, 7, and 8 we also show the unoccupied states. It is clear that the $4f$ dominated spectral features are due to an $f^1 \rightarrow f^2$ transition, in which multiplet effects are clearly visible. Since we have not found experimental BIS data for the heavy Ce pnictides our theory must be viewed as a prediction. We note that a calculation based on the LDA or LDA+U approximation would not result in spectral features displaying multiplet effects, and an experimental verification or rebuttal of the BIS data shown in Figs. 5, 6, 7, 8 would give valuable insight into which approximation is best for these systems. On general grounds however, one would expect for these materials that the Hubbard I approximation is better than LDA or LDA+U.

A similarity can be observed between the heavier Ce pnictides and γ-Ce. In the photoelectron spectrum of Ce both the γ-phase and the α-phase display the well screened $4f$ feature and the poor screened $4f$ feature, which for γ-Ce is located at about 2.0 eV binding energy[18,69]. γ-Ce is a localized $4f$ system, and therefore a Hubbard I calculation for γ-Ce should reproduce the lattice constant with equal accuracy as it does for the Ce pnictides. Our calculations for γ-Ce actually confirm this expectation and we obtain an equilibrium lattice constant of 9.56 a.u., 9.95 a.u, 9.78 a.u., respectively for PW91+HI, PBE96+HI, and AM05+HI. These values should be compared to the experimental lattice parameter which is equal to 9.75 a.u.[70], showing again that the AM05+HI approach results in the best agreement with experiment. For γ-Ce we have also calculated the bulk modulus to investigate if the lack of the well-screened $4f$ feature in the spectrum leads to a deficiency in more

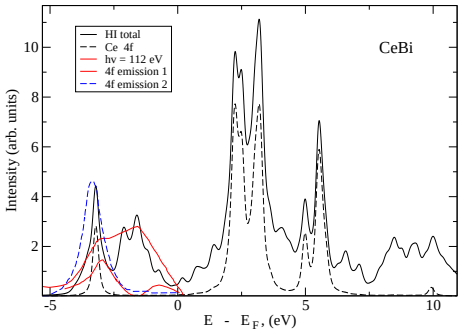

FIG. 8. (Color online) Experimental and calculated spectral properties of CeBi using the Hubbard I approximation. The total spectral function is labelled by the black solid line, while the Ce $4f$ contribution is marked by the black dashed line. The red dashed line and the red solid line respectively mark the experimental resonant $4f$ emission from Ref. 17 and the nonresonant emission, formed by the Bi $6p$ and Ce $5d$ states. The blue dashed line labels the resonant $4f$ emission from Ref. 18.

sensitive ground state properties than the lattice constant. We obtain a bulk modulus of 37 GPa, 31 GPa, and 27 GPa, respectively for PW91+HI, PBE96+HI, and AM05+HI. These values are in line with the GGA+U result of 34 GPa[71], and overestimate the experimental bulk modulus, which is equal to 19 GPa[71]. A better theory based on a more sophisticated approach would probably be able to correct this disagreement with the experiments.

IV. CONCLUSIONS

We conclude that the LDA/GGA+DMFT approach used in the present work with the SPTF and Hubbard I solvers gives very good values of lattice constants and acceptable spectral properties of Ce pnictides. The Hubbard I solver is not able to capture the experimental Kondo-like feature at the Fermi level observed for CeP, CeAs and CeSb, while for CeBi this peak is almost absent, and only a small shoulder is visible. This deficiency is inner to the method used, and may potentially be remedied with more sophisticated techniques such as quantum Monte-Carlo. However, in this case, technical problems of different nature may be introduced and related to the statistical noise of the Green's function. For reasonable computational resources the occupation numbers and the total energies would be less stable, and the spectral function would suffer of the uncertainty related to the maximum entropy method for analytical continuation. Finally it would also be problematic to include the spin-orbit coupling without arbitrarily discarding parts of the hybridization function.

It is interesting, nevertheless, that despite the inability of the Hubbard I approximation (or the SPTF solver) to capture the well-screened Kondo-like peak observed for some Ce pnictides the lattice constants are reproduced with a very good accuracy. This implies that the mechanism behind this feature does not contribute much to the chemical bonding. More sensitive properties as, e.g., the bulk modulus would probably show a signature of this discrepancy between theory and experiment, as verified in this paper for γ-Ce. It would be of a great interest to approach this problem with more refined methods, and this will be the aim of our future research.

Finally we also note that the lattice constants for the heavier Ce pnictides, in which the $4f$ states are essentially localized and non-bonding, can be well reproduced from a theory where these states are treated as core-states where they are not allowed to hop from lattice site to lattice site, and where hybridization to all other states is absent. Hence, a good alternative to treat the $4f$ states of localized $4f$ electron systems is to simply consider them as core like, which is an approximation that offers great computational speed with decent accuracy.

ACKNOWLEDGMENTS

We are very grateful to N. Mårtensson for the valuable discussions of the experimental data from the Ref. 17 and to M.I. Katsnelson and K. Held for discussions regarding the theoretical aspects of this work. The computations were performed on resources provided by the Swedish National Infrastructure for Computing (SNIC) at Uppsala Multidisciplinary Center for Advanced Computational Science (UPPMAX) and on resources provided by SNIC at the National Supercomputer Center (NSC) under the Project *matter2*. We acknowledge support from the Swedish Research Council. O.E. acknowledges support from the KAW foundation as well as the ERC (ASD - project 247062).

[1] B. Johansson, Phil. Mag. **30**, 469 (1974).
[2] J.M. Allen and R.M. Martin, Phys. Rev. Lett. **49**, 1106 (1982).
[3] D.C. Koskimaki, K.A. Gschneidner, Phys. Rev. B **11**, 4463 (1975).
[4] Ch.-G. Duan, R.F. Sabirianov, W.N. Mei, P.A. Dowben, S.S. Jaswal, and E.Y. Tsymbal, J. Phys.: Condens. Matter **19**, 315220 (2007).
[5] R. Didchenko and F.P. Gortsema, J. Phys. Chem. Solids **24**, 863 (1963).
[6] F. Patthey, S. Cattarinussi, W.-D. Schneider, Y. Baer, and B. Delley, Europhys. Lett. **2**, 883 (1986).
[7] F. Patthey, J.-M. Imer, W.-D. Schneider, H. Beck, and Y. Baer, Phys. Rev. B **42**, 8864 (1990).
[8] A. Delin, P. M. Oppeneer, M.S.S. Brooks, T. Kraft, J.M. Wills, B. Johansson, and O. Eriksson, Phys. Rev. B **55**, R10173 (1997).
[9] J. Schoenes, in Handbook on the Physics and Chemistry of the Actinides, edited by A.J. Freeman and G.H. Lander North- Holland, Amsterdam, 1984, Vol. 1, Chap. 5; J. Schoenes, in Moment Formation in Solids. Proceedings of the Nato Advanced Study Institute, edited by W.J.L. Buyers, Plenum, New York, 1984, p. 237.
[10] R.J. Birgeneau, E. Bucher, J.P. Maita, L. Passell, K.C. Turberfield, Phys. Rev. B **8**, 5345 (1973).
[11] B.R. Cooper, R. Siemmann, D. Yang, P. Thayamballi, and A. Banerjea, in Handbook on the Physics and Chemistry of the Actinides, edited by A.J. Freeman and G.H. Lander (North-Holland, Amsterdam, 1985), Vol. 2, Chap. 6, p. 435.
[12] B.R. Cooper, J. Less Common Met. **133**, 31 (1987).
[13] J. Rossat-Mignod, D. Delacote, J.M. Effantic, C. Vettier, O. Vogt, Physica B, **120**, 163 (1983).
[14] A. Schlegel, E. Kaldis, P. Wachter, and Ch. Zurcher, Phys. Lett. A **66**, 125 (1978).
[15] Y. Baer and Ch. Zürcher, Phys. Rev. Lett. **39**, 956 (1977).
[16] Y. Baer, R. Hauger, Ch. Zürcher, M. Campagna, G.K. Wertheim, Phys. Rev. B **18**, 4433 (1978).
[17] A. Franciosi, J.H. Weaver, N. Mårtensson, M. Croft, Phys. Rev. B **24**, 3651 (1981).
[18] J.W. Allen, S.-J. Oh, I. Lindau, J.M. Lawrence, L.I. Johansson, and S.B. Hagström, Phys. Rev. Lett. **46**, 1100

(1981).
[19] H. Kumigashira, H.-D. Kim, A. Ashihara, A. Chainani, T. Yokoya, T. Takahashi, A. Uesawa, and T. Suzuki, Phys. Rev. B **56**, 13654 (1997).
[20] M. Croft, A. Franciosi, J.H. Weaver, A. Jayaraman, Phys. Rev. B **24**, 544 (1981)
[21] W. Gudat, M. Campagna, R. Rosei, J.H. Weaver, W. Eberhardt, F. Hulliger, and E. Kaldis, J. Appl. Phys. **52**, 2123 (1981).
[22] O. Gunnarsson and K. Schonhammer, Phys. Rev. B **28**, 4315 (1983).
[23] J.C. Fuggle, M. Campagna, Z. Zolnierek, R. Lässer, and A. Platau, Phys. Rev. Lett. **45**, 1597 (1980).
[24] J.W. Allen, S.-J. Oh, M.B. Maple, M.S. Torikachvili, Phys. Rev. B **28**, 5347 (1983).
[25] N. Mårtensson, B. Reihl, R.D. Parks, Solid State Communications **41**, 573 (1982).
[26] M.R. Norman, D.D. Koelling, A.J. Freeman, H.J.F. Jansen, B.I. Min, T. Oguchi, and Ling Ye, Phys. Rev. Lett. **53**, 1673 (1984).
[27] S.H. Liu, K.-M. Ho, Phys. Rev. B **28**, 4220 (1983).
[28] V. Kanchana, G. Vaitheeswaran, Xinxin Zhang, Yanming Ma, A. Svane, and O. Eriksson, Phys. Rev. B **84**, 205135 (2011)
[29] T. Kotani, M. van Schilfgaarde, and S.V. Faleev, Phys. Rev. B **76**, 165106 (2007).
[30] J.M. Wills and B.R. Cooper, Phys. Rev. B **36**, 3809 (1987).
[31] J. Laegsgaard and A. Svane, Phys. Rev. B **58**, 12817 (1998).
[32] O. Sakai and Yu. Shimizu, J. Phys. Soc. Japan **76**, 044707 (2007).
[33] O. Sakai, Yu. Shimizu, and Ya. Kaneta, J. Phys. Soc. Japan **74**, 2517 (2005).
[34] A. Grechnev, I. Di Marco, M.I. Katsnelson, A.I. Lichtenstein, J. Wills, and O. Eriksson, Phys. Rev. B **76**, 035107 (2007).
[35] I. Di Marco, J. Minar, S. Chadov, M.I. Katsnelson, H. Ebert, and A.I. Lichtenstein, Phys. Rev. B **79**, 115111 (2009).
[36] P. Thunström, I. Di Marco, A. Grechnev, S. Lebegue, M.I. Katsnelson, A. Svane, and O. Eriksson, Phys. Rev. B **79**, 165104 (2009).
[37] O. Grånäs, I. Di Marco, P. Thunström, L. Nordström, O. Eriksson, T. Björkman, J.M. Wills, Computational Materials Science **55**, 295 (2012).
[38] P. Hohenberg and W. Kohn, Phys. Rev. **136**, B864 (1964).
[39] W. Kohn and L. Sham, Phys. Rev. **140**, A1133 (1965).
[40] A.I. Lichtenstein and M.I. Katsnelson, Phys. Rev. B **57**, 6884 (1998).
[41] V.I. Anisimovy, A.I. Poteryaevy, M.A. Korotiny, A.O. Anokhiny, and G. Kotliar, J. Phys. Condens. Matter **9**, 7359 (1997).
[42] A. Georges, G. Kotliar, W. Krauth, and M.J. Rozenberg, Rev. Mod. Phys. **68**, 13 (1996).
[43] G. Kotliar, S.Y. Savrasov, K. Haule, V.S. Oudovenko, O. Parcollet and C.A. Marianetti, Rev. Mod. Phys. **78**, 865 (2006).
[44] K. Held, Adv. Phys. **56**, 829 (2007).
[45] J.P. Perdew and Y. Wang, Phys. Rev. B **45**, 13244 (1992).
[46] J.P. Perdew, K. Burke, M. Ernzerhof, Phys. Rev. Lett. **77**, 3865 (1996).
[47] R. Armiento and A.E. Mattsson, Phys. Rev. B **72**, 085108 (2005).
[48] O.K. Andersen, Phys. Rev. B **12**, 3060 (1975).
[49] J.M. Wills, O. Eriksson, M. Alouani, and D.L. Price, "Full-Potential LMTO Total Energy and Force Calculations" in *Elecytronic structure and physical properties of solids* Ed. Hugues Dreysse, Springer Verlag, Berlin (2000) p.148; J.M. Wills, M. Alouani, P. Andersson, A. Delin, O. Eriksson, O. Grechnev, "Full-Potential Electronic structure method" Springer, Berlin, (2010).
[50] M.I. Katsnelson and A.I. Lichtenstein, Eur. Phys. J. B, **30**, 9 (2002).
[51] L.V. Pourovskii, M.I. Katsnelson, and A.I. Lichtenstein, Phys. Rev. B **72**, 115106 (2005).
[52] J. Hubbard, Proc. R. Soc. London, Ser. A **276**, 238 (1963); J. Hubbard, Proc. R. Soc. London, Ser. A **277**, 237 (1964); J. Hubbard, Proc. R. Soc. London, Ser. A **281**, 401 (1964); J. Hubbard, Proc. R. Soc. London, Ser. A **285**, 542 (1965).
[53] K. Haule, Ch.-H. Yee, and K. Kim, Phys. Rev. B **81**, 195107 (2010).
[54] I. Di Marco, J. Minár, J. Braun, M.I. Katsnelson, A. Grechnev, H. Ebert, A.I. Lichtenstein, and O. Eriksson, Eur. Phys. J. B **72**, 473 (2009).
[55] J. Sánchez-Barriga, J. Fink, V. Boni, I. Di Marco, J. Braun, J. Minár, A. Varykhalov, O. Rader, V. Bellini, F. Manghi, H. Ebert, M.I. Katsnelson, A.I. Lichtenstein, O. Eriksson, W. Eberhardt, and H. A. Dürr Phys. Rev. Lett. **103**, 267203 (2009)
[56] H. Kumigashira, S.-H. Yang, T. Yokoya, A. Chainani, T. Takahashi, A. Uesawa, and T. Suzuki, Phys. Rev. B **55**, R3355 (1997).
[57] P.G. Baym and L. Kadanoff Phys. Rev. B **124**, 287 (1961).
[58] V. Drchal, V. Janis, J. Kudrnovsky, V.S. Oudovenko, X. Dai, K. Haule, and G. Kotliar, J. Phys.: Condens. Matter **17**, 61 (2005).
[59] I. Di Marco, P. Thunström, L. Pourovskii, O. Grånäs, L. Nordström, M. I. Katsnelson, and O. Eriksson, *in preparation.*
[60] W. Gudat, R. Rosei, J.H. Weaver, E. Kaldis and F. Hulliger, Solid State Comm. **41**, 37 (1982).
[61] J.M. Leger, D. Ravot, J. Rossat-Mignod, J. Phys. C. Solid State Phys. **17**, 4935 (1984).
[62] A. Svane, Z. Szotek, W.M. Temmerman, J. Lagsgaard, and H. Winter, J. Phys. Condens. Matter **10**, 5309 (1998).
[63] G.L. Olcese, J. Phys. F: Metal Phys. **9**, 569 (1979).
[64] M.S.S. Brooks, J. Magn. Magn. Mat. **47**, 260 (1985).
[65] F. Hulliger and H.R. Ott, Z. Physik B **29**, 47 (1978).
[66] R.P.C. Schram, J.G. Boshoven, E.H.P. Cordfunke, R.J.M. Konings, R.R. van der Laan, J. Alloys and Comp. **252**, 20 (1997).
[67] Ch.-G. Duan, R.F. Sabirianov, W.N. Mei, P.A. Dowben, S.S. Jaswal, and E.Y. Tsymbal, J. Phys.: Condens. Matter **19**, 315220 (2007).
[68] E. Wuilloud, B. Delley, W.-D. Schneider, Y. Baer, J. Magn. Magn. Mat. **47**, 197 (1985).
[69] D.M. Wieliczka, C.G. Olson, and D.W. Lynch, Phys. Rev. B **29**, 3028 (1984).
[70] B.J. Beaudry and P.E. Palmer, J. Less-Common Metals **34**, 225 (1974); D.C. Koskimaki, K.A. Gschneider Jr., and N.T. Panousis, J. Crystal Growth **22**, 225 (1974).
[71] B. Amadon, F. Jollet, and M. Torrent, Phys. Rev. B **77**, 155104 (2008)